Eur. J. Mech. B - Fluids 19 (2000) 855–870

S0997-7546(00)00134-5/FLA

A new method for the calculation of steady periodic capillary-gravity waves on water of arbitrary uniform depth

Mohammed Debiane [a], Christian Kharif [b,*], Mustapha Amaouche [a]

[a] *Université des Sciences et de la Technologie Houari Boumediene, B.P. 32, El Alia, Alger, Algeria*
[b] *Institut de Recherche sur les Phénomènes Hors Equilibre / Laboratoire I.O.A., 163 avenue de Luminy - case 903, 13288 Marseille cedex 9, France*

(Received 27 September 1999; revised 23 March 2000; accepted 11 April 2000)

Abstract – This paper presents a method for the calculation of steady periodic capillary-gravity waves on water of arbitrary uniform depth. The method developed by Debiane and Kharif in 1997 for infinite depth is extended to finite depth. The water-wave problem is reduced to a system of nonlinear algebraic equations which is solved using Newton's method. For the resonant configurations, the method does not suffer from the Wilton's failures and is valid for all depths. In addition, it is shown that the method allows the computation of solitary waves and generalized solitary waves. © 2000 Éditions scientifiques et médicales Elsevier SAS

capillary-gravity waves / water wave problem / Newton's method

1. Introduction

The problem of periodic capillary-gravity waves on deep water has been the subject of a substantial literature. However much less work appears to have been done on the corresponding problem when the depth is finite. Furthermore, most of the research on finite depth case has concentrated either on small amplitude Wilton ripples or on solitary waves.

Works devoted to Wilton ripples have been performed by Kamesvara Rav [1], Barakat and Houston [2] and Nayfeh [3]. The solutions have concentrated on second or third harmonic resonance and are limited to the second or the third order. They are based on perturbation expansion methods which render access to higher orders difficult owing to the amount of algebra involved.

Capillary-gravity waves on water of finite depth have been also calculated by Hunter and Vanden-Broeck [4] and Zufiria [5] but these papers are largely concerned by solitary waves. Such waves are obtained as solutions of a generalized Korteweg–de Vries equation. Hunter and Vanden-Broeck, in addition, also used a numerical scheme based on an integro-diferential equation formulation to compute solitary waves solutions and long wave length periodic solutions of the full equations. Iooss and Kirchgässner [6] proved the existence of two families of solitary waves considered as depression and elevation waves. These waves bifurcate from a uniform flow or from infinitesimal periodic waves when phase and group velocities are equal to each other. More recently, Dias et al. [7] produced a paper covering a large variety of bifurcation curves revealing the presence of turning points along some of them.

* Correspondence and reprints; e-mail: Kharif@pollux.univ-mrs.fr

Jones [8] provided a proof of the existence of small amplitude solutions for the periodic capillary-gravity wave problem of finite depth. He also determined the values of the phase speed for which a branch of waves may bifurcate from the uniform horizontal flow.

Pure capillary waves on water of finite depth have been investigated by Kinnersley [9] who derived an exact solution in terms of elliptic functions. Also, accurate numerical calculations of these waves have been carried out by Bloor [10] who used an integro-diferential equation formulation.

Recently, Debiane and Kharif [11] extended the method developed by Longuet-Higgins [12,13] for the computation of gravity waves on deep water to the corresponding problem taking into account the surface tension. Motivated by the efficiency of this method, we develop here a similar method for the uniform depth problem. The algorithm, easy to implement on computers, gives accurate results and gives solutions for almost all the permissible values of the relevant parameters. The power and simplicity of the method are perhaps more obvious in the computations of special solutions, such as resonant waves, generalized solitary waves and limiting forms, where no extra work is needed. One would add that Balk [14] showed that the system of quadratic equations discovered by Longuet-Higgins can be derived from the canonical system of Lagrange equations.

In section 2 the set of integral equations given by Longuet-Higgins is reduced to a system of nonlinear algebraic equations in which the term corresponding to the effects of surface tension is expressed as a simple function of the slope of the local tangent. The numerical procedure is described in section 3. In section 4 we give the expressions of some integral properties and results are presented in section 5.

2. Calculation of the coefficients

The analysis proceeds along the lines of the deep-water case (Debiane and Kharif [11]), with introduction of the bottom effect. We consider capillary-gravity waves on the free surface of a liquid layer of uniform depth. The fluid is taken to be homogeneous, incompressible and inviscid, and the motion is assumed to be irrotational. One considers two-dimensional periodic symmetric waves propagating without change of shape at constant phase speed c. The phase speed c is measured relative to a reference frame in which the time-mean value of the horizontal fluid velocity vanishes at any fixed point below the wave troughs. Let x and y be horizontal and vertical co-ordinates in a reference frame moving with the wave at the speed c. In this reference frame the wave is steady. Units of length and time are chosen such as the wave number and the body acceleration are equal to unity. The origin is fixed above a crest at such a distance that Bernoulli's equation, at the free surface, can be written as

$$q^2 + 2\eta - 2\kappa \frac{\eta_{xx}}{(1+\eta_x^2)^{3/2}} = 0, \tag{1}$$

where $\eta(x)$ is the free surface level, q the particle velocity and κ is the dimensionless capillary number (the inverse of the Bond number) defined by:

$$\kappa = \frac{k^2\tau}{\rho g}.$$

Here g is the acceleration due to gravity, k the wave number, and τ and ρ are the surface tension and the density of the fluid, respectively.

The flow is further simplified if the potential function $\phi(x, y)$ and the stream function $\psi(x, y)$ are used as independent variables. The stream function takes the values $\psi = 0$ at the free surface and $\psi = \psi_B$ at the bottom. We may then write

$$x = -\frac{\phi}{c} - \sum_{n=1}^{\infty} A_n \cosh\frac{n(\Psi_B - \Psi)}{c} \sin\frac{n\phi}{c}, \tag{2a}$$

$$y = -\frac{\Psi}{c} + \frac{A_0}{2} + \sum_{n=1}^{\infty} A_n \sinh\frac{n\,(\Psi_B - \Psi)}{c} \cos\frac{n\phi}{c}. \tag{2b}$$

Since the streamfunction ψ is chosen to be zero on the free surface, the equation of the free surface can therefore be expressed parametrically in the form

$$x = -\varphi - \sum_{n=1}^{\infty} \gamma_n a_n \sin n\varphi, \tag{3a}$$

$$\eta = \frac{a_0}{2} + \sum_{n=1}^{\infty} a_n \cos n\varphi, \tag{3b}$$

where we have written

$$\varphi = \frac{\phi}{c}; \quad a_0 = A_0; \quad a_n = A_n \sinh nd; \quad \gamma_n = \coth nd; \quad \gamma_0 = 1; \quad d = \frac{\Psi_B}{c}.$$

For a fixed value of d, the coefficients a_n $(n = 0, 1, 2, \ldots)$ are derived from the following set of integral relations given by Longuet-Higgins [12,15]

$$\int_0^{-2\pi} q^2 (x_\varphi + i\gamma_j \eta_\varphi) \mathrm{e}^{-ij\varphi}\, \mathrm{d}\varphi = 0 \quad (j = 1, 2, 3 \ldots) \tag{4}$$

combined with the relation defining the dimensionless mean depth H

$$H = -y_B + \bar{\eta} = d + \frac{1}{2}\sum_{n=1}^{\infty} \alpha_n a_n^2. \tag{5}$$

Here y_B is the value of y at the bottom, $\bar{\eta}$ the (Eulerian) mean level and $\alpha_n = n\gamma_n$.

Using (1), the integral of equation (4), say I_j, can be written as

$$I_j = I_j^{(1)} + I_j^{(2)} \tag{6a}$$

with

$$I_j^{(1)} = -2\int_0^{-2\pi} \eta (x_\varphi + i\gamma_j \eta_\varphi) \mathrm{e}^{-ij\varphi}\, \mathrm{d}\varphi \tag{6b}$$

and

$$I_j^{(2)} = 2\kappa \int_0^{-2\pi} \frac{\eta_{xx}}{(1+\eta_x^2)^{3/2}} (x_\varphi + i\gamma_j \eta_\varphi) \mathrm{e}^{-ij\varphi}\, \mathrm{d}\varphi. \tag{6c}$$

Using (3a) and (3b), and carrying out the integration of $I_j^{(1)}$ we obtain

$$I_j^{(1)} = -2\pi \left\{ a_j + \frac{1}{2}\sum_{m=1}^{\infty} \alpha_m a_m (a_{m+j} + a_{|m-j|}) - \frac{1}{2}\gamma_j \sum_{m=1}^{\infty} m a_m (a_{m+j} - a_{|m-j|}) \right\}. \tag{7}$$

$I_j^{(2)}$, which has to be evaluated on the free surface $\psi = 0$, may be written in the form

$$I_j^{(2)} = 2\kappa \int_0^{-2\pi} \eta_{x\varphi} \frac{1 + i\gamma_j \eta_x}{(1+\eta_x^2)^{3/2}} \mathrm{e}^{-ij\varphi}\, \mathrm{d}\varphi.$$

Integrating by parts, we obtain

$$I_j^{(2)} = -2\kappa i \left[\frac{\gamma_j + i\eta_x}{(1+\eta_x^2)^{1/2}} \mathrm{e}^{-ij\varphi} \right]_0^{-2\pi} + 2\kappa j \int_0^{-2\pi} \frac{\gamma_j + i\eta_x}{(1+\eta_x^2)^{1/2}} \mathrm{e}^{-ij\varphi}\, \mathrm{d}\varphi. \tag{8}$$

The first term on the right-hand side vanishes due to periodicity. To proceed further let us introduce the following Fourier expansion

$$\mathrm{e}^{i\theta} = \frac{1 + i\eta_x}{(1+\eta_x^2)^{1/2}} = \frac{C_0}{2} + \sum_{n=1}^{\infty} (C_n \cos n\varphi + i S_n \sin n\varphi), \tag{9}$$

where $\theta = \tan^{-1}(\eta_x)$ is the tilting angle of the local tangent to the wave with respect to the horizontal line. It should be noted that

$$\int_0^{-2\pi} \mathrm{e}^{i\theta} \mathrm{e}^{-ij\varphi}\, \mathrm{d}\varphi = -\pi (C_j + S_j),$$

thus equation (8) becomes

$$I_j^{(2)} = -2\pi j \kappa (\gamma_j C_j + S_j). \tag{10}$$

This expression, as a function of θ, avoids the singularities introduced by η_x in the profiles presenting infinite slopes at some points.

The resulting expression of I_j is then

$$I_j = -2\pi \left\{ a_j + \frac{1}{2} \sum_{m=1}^{\infty} \alpha_m a_m (a_{m+j} + a_{|m-j|}) - \frac{1}{2} \gamma_j \sum_{m=1}^{\infty} m a_m (a_{m+j} - a_{|m-j|}) + j\kappa (\gamma_j C_j + S_j) \right\}. \tag{11}$$

Finally equations (4) can be written as

$$2a_j + \sum_{m=1}^{\infty} \alpha_m a_m (a_{m+j} + a_{|m-j|}) - \gamma_j \sum_{m=1}^{\infty} m a_m (a_{m+j} - a_{|m-j|}) + 2j\kappa (\gamma_j C_j + S_j) = 0$$
$$(j = 1, 2, 3, \ldots). \tag{12}$$

In the case of gravity waves ($\kappa = 0$), this system of equations reduces to equations (6.6) of Longuet-Higgins [15], and for capillary-gravity waves on water of infinite depth ($\gamma_n = 1$ with $n = 1, 2, \ldots$), we obtain equations (11a) of Debiane and Kharif [11].

3. Numerical procedure

The series in (3a) and (3b) are truncated at N. Integer N is increased until convergence of the solutions is reached. N is chosen as small as possible provided that further increase in its value will not significantly change

the solutions. Therefore, the resulting system may be written:

$$F_j\big(a_n(n=0,\ldots,N)\big)=0,\quad j=1,\ldots,N+1. \tag{13}$$

Expressions F_j correspond to (12) for $j=1,\ldots,N$ and F_{N+1} to (5).

The present method can also be applied for fixed values of the wave steepness ε by using, instead of equation (5), the following relationship

$$\varepsilon=\frac{1}{2}(\eta_{\text{crest}}-\eta_{\text{trough}})\approx\sum_{n=0}^{(N-1)/2}a_{2n+1}.$$

In this case, d may be calculated at each iteration using (5).

The system of nonlinear equations (13) is solved by Newton's method which iterates, with quadratic convergence, from an initial approximation. For high wave steepness five iterations are required to satisfy the system of equations with an error less than 10^{-14}. In order to determine the increments of the coefficients in Newton's method it is necessary to calculate the Jacobian matrix from the following equations: for $j=1,\ldots,N$

$$\frac{\partial F_j}{\partial a_l}=\begin{cases}2\alpha_j a_j & (l=0),\\ 2\delta_{jl}+(\alpha_j+\alpha_l+\alpha_{j+l})a_{j+l}+(\alpha_j+\alpha_l+\alpha_{|j-l|})a_{|j-l|}+2\kappa\left(\alpha_j\dfrac{\partial C_j}{\partial a_l}+j\dfrac{\partial S_j}{\partial a_l}\right) & (l\neq 0),\end{cases} \tag{14a}$$

and for $j=N+1$

$$\frac{\partial F_{N+1}}{\partial a_l}=\begin{cases}0 & (l=0),\\ \alpha_l a_l & (l\neq 0).\end{cases} \tag{14b}$$

Introducing Fourier expansions we can compute the derivatives of C_j and S_j in the following manner:

$$-\sin\theta\frac{x_\varphi+\eta_\varphi}{x_\varphi^2+\eta_\varphi^2}=\frac{A_0}{2}+\sum_{n=1}^{\infty}(A_n\cos n\varphi+B_n\sin n\varphi), \tag{15a}$$

$$\cos\theta\frac{x_\varphi+\eta_\varphi}{x_\varphi^2+\eta_\varphi^2}=\frac{A_0^*}{2}+\sum_{n=1}^{\infty}\big(A_n^*\cos n\varphi+B_n^*\sin n\varphi\big), \tag{15b}$$

which give

$$\frac{\partial C_j}{\partial a_m}=\frac{\alpha_k}{2}(A_{|m-j|}+A_{m+j})-\frac{m}{2}(B_{m-j}+B_{m+j}),$$

$$\frac{\partial S_j}{\partial a_m}=\frac{\alpha_m}{2}(B_{j-m}^*+B_{j+m}^*)-\frac{m}{2}(A_{|j-m|}^*-A_{J+m}^*),$$

where we have the set

$$B_{-n}=-B_n;\qquad B_{-n}^*=-B_n^*.$$

There are several methods for calculating Fourier coefficients in (9), (15a) and (15b). The use of Fast Fourier Transform (F.F.T.) was found to work well with adequate sampling. If the domain of variable $\varphi\in[-2\pi,0]$ is

divided into M intervals and the series (3a) and (3b) are truncated at N, then M and N may be chosen with a weak constraint, i.e. $M > 2N$ in order to avoid the aliasing phenomenon.

To compute

$$\theta_i = \theta(\varphi_i),$$

where

$$\varphi_i = -\frac{i-1}{M}2\pi \quad (i = 1, 2, 3, \ldots, M+1),$$

we may write

$$\theta_i = \tan^{-1}\eta_x(\varphi_i) = \tan^{-1}\left(\frac{\eta_\varphi}{x_\varphi}\right)_{\varphi=\varphi_i}$$

and use (3a) and (3b). The singularities introduced by infinite values of η_x may be located at points where x_ϕ vanishes. Then, according to this location, we assign to θ one of the following values:$-3\frac{\pi}{2}, -\frac{\pi}{2}, \frac{\pi}{2}, 3\frac{\pi}{2}$.

4. Integral properties

The solutions given by the previous method may be used to provide several integral properties of the motion such as phase velocity and kinetic and potential energies.

If q_0 denotes the value of q at $x = 0$ which corresponds to location of the crest, the phase velocity c can be derived from the relation

$$c = q_0 x_\varphi(0). \tag{16}$$

From (1) we have

$$q_0^2 = -2\eta(0) + 2\kappa\frac{\eta_{xx}(0)}{(1+\eta_x^2(0))^{3/2}}. \tag{17}$$

Let us note that

$$\eta_x(0) = 0,$$

$$\eta_{xx}(0) = \frac{\eta_{\varphi\varphi}(0)}{x_\varphi^2(0)}.$$

Thus, it follows, from (16) and (17), that

$$c^2 = -2\eta(0)x_\varphi^2(0) + 2\kappa\eta_{\varphi\varphi}(0),$$

and using (3a) and (3b) we find

$$c^2 = -2\left(\frac{a_0}{2} + \sum_{n=1}^{\infty} a_n\right)\left(-1 - \sum_{n=1}^{\infty}\alpha_n a_n\right)^2 - 2\kappa\sum_{n=1}^{\infty} n^2 a_n. \tag{18}$$

To calculate the potential and kinetic energies we choose the x-axis so that the origin is at the mean level. It is similar to substitute $a_0/2$ for $-b_0$ in equation (3b) with

$$b_0 = \frac{1}{2}\sum_{n=1}^{\infty} \alpha_n a_n^2.$$

Following Longuet-Higgins [13], the kinetic energy can be calculated in the form

$$T = \frac{1}{2} c^2 b_0. \tag{19}$$

The potential energy is given by

$$V = \frac{1}{2}\overline{\eta^2} + \kappa\left[\overline{(1+\eta_x^2)^{1/2} - 1}\right] = V_g + V_\tau.$$

The overbar means averaging over a wavelength. The gravity and capillary parts of the potential energy are respectively V_g and V_τ. The potential energy V_g due to gravity alone is defined as

$$\begin{aligned} V_g &= \frac{1}{4\pi}\int_0^{2\pi} \eta^2 \,\mathrm{d}x = \frac{1}{4\pi}\int_0^{-2\pi} \eta^2 x_\varphi \,\mathrm{d}\varphi \\ &= \frac{1}{4\pi}\int_0^{-2\pi} \left(-b_0 + \sum_{n=1}^{\infty} a_n \cos n\varphi\right)^2 \left(-1 - \sum_{n=1}^{\infty} \alpha_n a_n \cos n\varphi\right) \mathrm{d}\varphi. \end{aligned}$$

Using the properties of Fourier series products we obtain

$$V_g = \frac{1}{4}\omega_0 + \frac{1}{4}\sum_{m=1}^{\infty} \alpha_m a_m \omega_m, \tag{20a}$$

where

$$\begin{aligned} \omega_0 &= 2b_0^2 + \sum_{n=1}^{\infty} a_n^2, \\ \omega_m &= -b_0 a_m + \frac{1}{2}\sum_{n=1}^{\infty} a_n (a_{m+n} + a_{|m-n|}). \end{aligned} \tag{20b}$$

The potential energy V_τ due to surface tension alone is given by

$$V_\tau = \kappa\left[\frac{1}{2\pi}\int_0^{2\pi} \left(1+\eta_x^2\right)^{1/2} \mathrm{d}x - 1\right] = \kappa\left\{\frac{1}{2\pi}\int_0^{2\pi} \left[(1+i\eta_x)(1+\eta_x^2)^{-1/2}\right](1-i\eta_x)\,\mathrm{d}x - 1\right\}.$$

The term in square brackets is equal to the complex $\mathrm{e}^{i\theta}$ and its Fourier expansion is given by (9). Then we may write V_τ as follows

$$V_\tau = \kappa\left\{\frac{1}{2\pi}\int_0^{-2\pi} \left[\frac{C_0}{2} + \sum_{n=1}^{\infty} (C_n \cos n\varphi + i S_n \sin n\varphi)\right](x_\varphi - i\eta_\varphi)\,\mathrm{d}\varphi - 1\right\}.$$

Using the relationships (3a) and (3b) with the properties of Fourier series products we get

$$V_\tau = \frac{\kappa}{2}\left[C_0 + \sum_{n=1}^{\infty}(\alpha_n a_n C_n + n a_n S_n) - 2\right]. \tag{21}$$

5. Results and discussion

Solutions of equations (13) are computed for given values of κ and H, by decreasing d from $d \approx H$ to the limiting value. CPU time and convergence rates are similar to those of the deep water case. Our computations lies on the region of the two parameter space $H-\kappa$ in which H varies from 10^{-4} to 10^{10} and κ from 0 to 10^{10}. Taking $H = 10^{10}$, the method is in full agreement with that of Debiane and Kharif [11]. In the case of finite depth, the results of Bloor [10] are taken as reference for comparison. For $\kappa = 10^{10}$, *figure 1* shows a plot of ε against c^2/κ. The curves are labeled, as did Bloor, for constant values of the shallowness h/λ, where h is the dimensional depth and λ the wavelength. The figure is very similar to figure 4 produced by Bloor. One emphasizes that H is the normalized mean depth relative to the inverse of the wavenumber.

Before discussing our results, it is worth noting that there is a plethora of solutions corresponding to waves of different type. They depend on wave parameters such as the height, wave speed, depth H and the inverse of the Bond number κ. Obviously, it is not an easy task to provide a complete analysis taking into account the effect of all the parameters. Furthermore the problem is made more complicated by the existence of the multiplicity of the solutions coming from the interaction between two modes. Owing to this difficulty, in this section we analyze only some effects of the depth and surface tension. To illustrate the efficiency of the present method we shall provide results corresponding to special cases as those obtained for resonant and solitary waves.

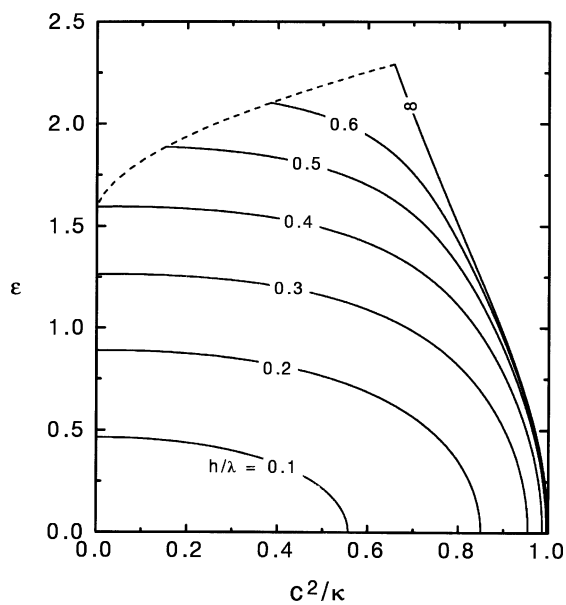

Figure 1. Variation of wave speed with amplitude for capillary waves ($\kappa = 10^{10}$).

5.1. Moderate depth

First we consider the effect of the depth on the regular (uniform) wave trains. The value of $\kappa = 1$ may be convenient to analyze this effect. *Figure 2* shows the variation of the wave speed with steepness for various values of h/λ. Also shown in this figure the curve (dashed line) referring to the limiting waves when two adjacent crests entrap a bubble at the trough. Thus the curves $h/\lambda =$ constant which intersect this line have an ultimate profile with a bubble at the trough. They correspond to highest values of h/λ and when the depth decreases, beyond some critical value h^*/λ, the shape of the trough of the limiting waves distorts gradually until it presents a sharp corner. This change of topology is shown in *figure 3* where the scales have been enlarged to emphasize this behavior. This critical value of the shallowness seems to correspond to the curve $h^*/\lambda =$ constant which pass through the intersection of the dashed line with the axis $c^2/\lambda = 0$. This curve separates the region of solutions (say class I) having qualitatively the behavior of capillary-gravity waves propagating in infinite depth from the region where this similarity stops. The latter corresponds to another class (say class II) of waves. *Figure 4* displays typical profiles of waves of class II. It was noted that the distance between troughs and bottom decreases but the distance below the trough does not vanish. For the case of waves of class II, the criterion for the limiting configurations remains to be defined. Indeed, for these waves the enclosed bubble criterion is inapplicable along with the sharp corner criterion that has to be excluded owing to the surface tension. However, from detailed calculations, it has been observed that, as we approach the limiting configuration, the steepness appears to converge to a finite value and the phase velocity to zero. Unfortunately, this apparent limiting configuration could not be achieved by our method. Indeed, the approach to the limiting configuration involves the use of a decrement Δd, with respect to d, becoming smaller and smaller. Hence, as criterion we chose to stop the computation process when Δd reaches a value that generates a variation of the steepness $\Delta\varepsilon$ less than 10^{-10}. In general this criterion gives a value of $c \approx 10^{-3}$.

For fixed values of c and h/λ, one can note from comparison between *figures 1* and *2* that the amplitude increases as κ increases. The effect of the depth on the wave steepness, ε, is more complicated to analyze. These figures suggest that the amplitude increases as depth increases. Nevertheless this is not a general feature

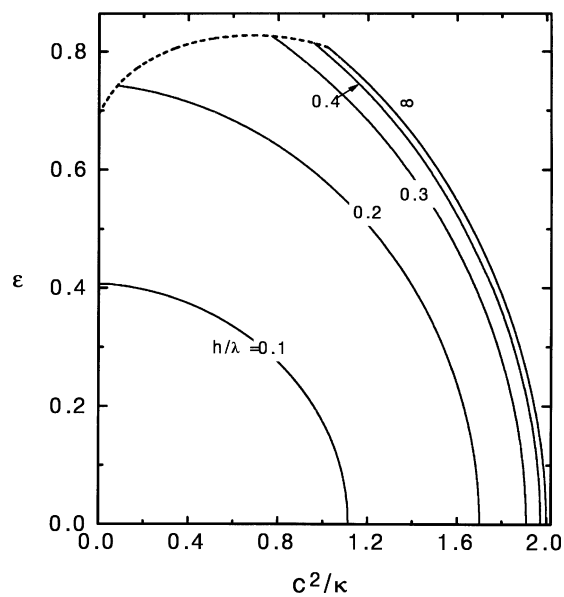

Figure 2. Variation of wave speed with amplitude for $\kappa = 1$.

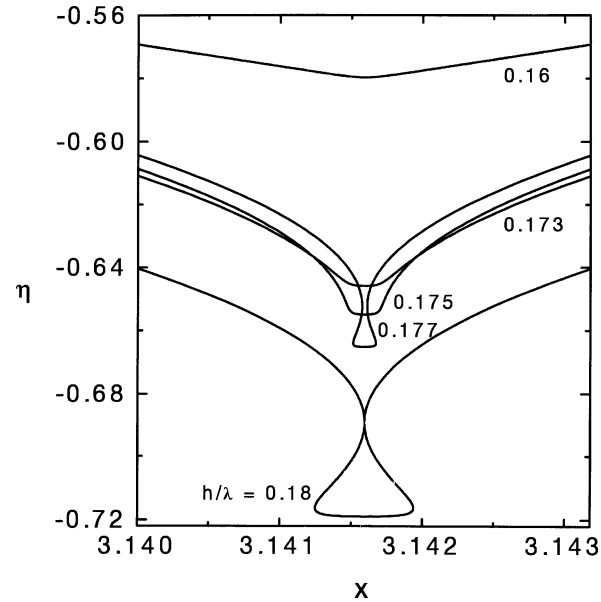

Figure 3. Evolution of the shape of the trough of the highest wave for h/λ close to $h^*/\lambda \approx 0.18$ and $\kappa = 1$.

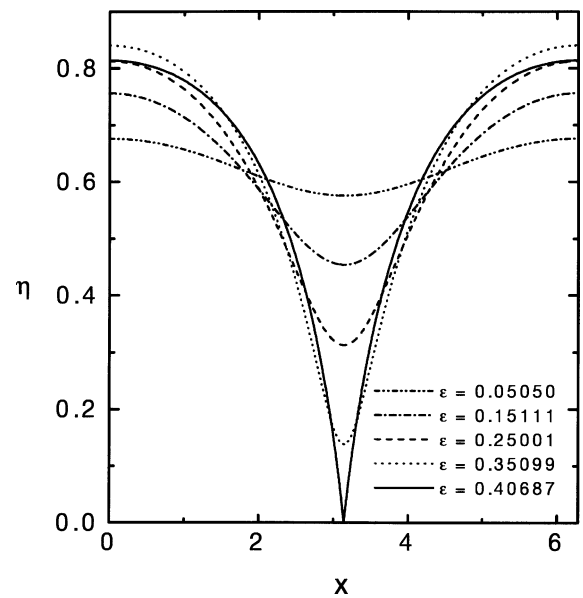

Figure 4. Wave profiles of waves of class II for $\kappa = 1$ and $h/\lambda = 0.1$. The origin is on the bottom.

because in many cases ε is modified by the presence of secondary crests or/and troughs and is not the true steepness.

For $\kappa = 1$ and $h/\lambda = (0.1, 0.3)$, the plots of the kinetic energy T, the potential energy due to the gravity V_g, and the potential energy due to the surface tension V_τ as a function of d are shown in *figure 5*. Let us consider first the kinetic energy. In deep water for large values of κ, it was found (Hogan [16]) that the kinetic energy increases monotonically with ε (or equivalently with decreasing d). For small values of κ (few units or less) the

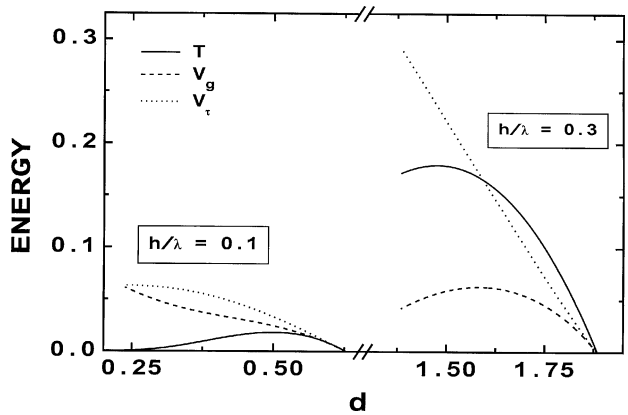

Figure 5. Kinetic and potential energies versus d for $\kappa = 1$ and $h/\lambda = 0.1, 0.3$.

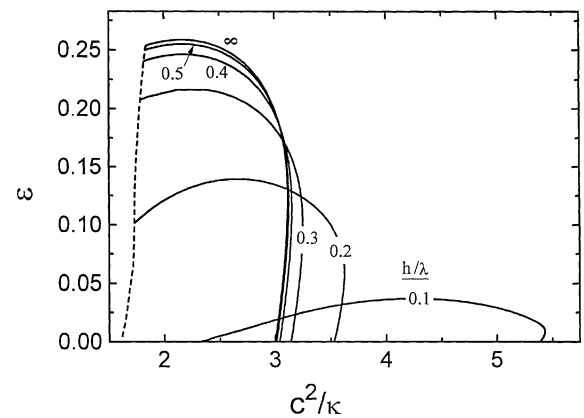

(a)

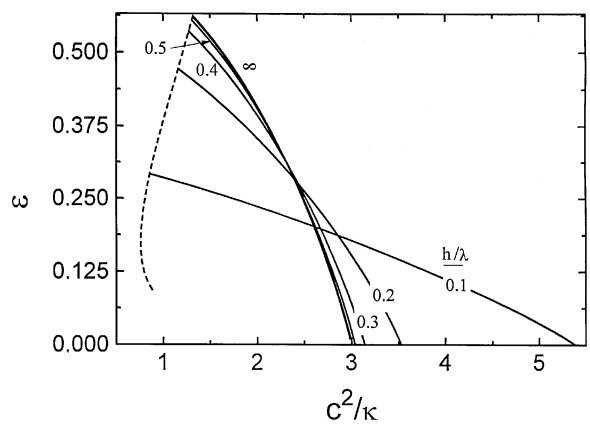

(b)

Figure 6. Variation of wave speed with amplitude in the case of resonant waves for $m = 2$. (a) Gravity-like type, (b) capillary-like type.

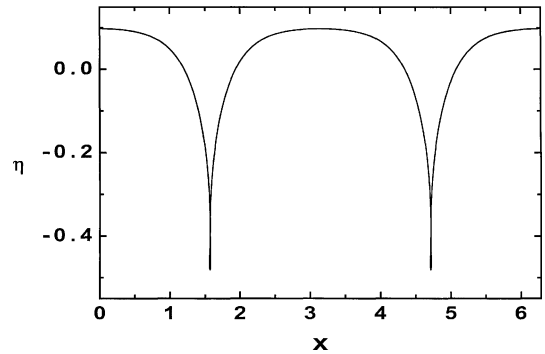

Figure 7. Limiting wave profile of gravity-like type in the case of resonant waves for $m = 2$, $h/\lambda = 0.1$ ($\kappa = 0.1152956$), $\varepsilon = 0$ and $d = 0.479303$.

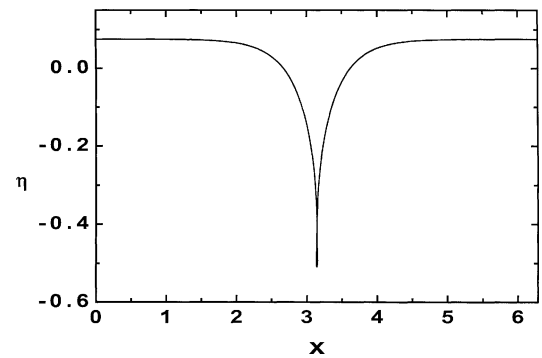

Figure 8. Limiting wave profile of capillary-like type in the case of resonant waves for $m = 2$, $h/\lambda = 0.1$ ($\kappa = 0.1152956$), $\varepsilon = 0.29205$ and $d = 0.524325$.

curves display maxima in the neighborhood of the limiting amplitude. For finite depth, maxima are found for all values of κ and their location moves to the region of large d when the depth is decreased. The general form of these curves is nearly parabolic for high values of the depth and when the depth decreases the left branch moves down until it reaches the horizontal axis becoming progressively flattened. Next we focus on the curves of the potential energy. For infinite depth, V_g as a function of d was found to have a well-defined maximum before the limiting profile is achieved. As the depth decreases, the left branch stands up progressively and when h/λ becomes smaller than h^*/λ the curves exhibit an inflexion point instead of a maximum. This behavior may be related to the sharpening of the trough of the wave profile when h/λ is decreased. For high values of h/λ the curves of V_τ exhibit an inflexion point and for h/λ less than h^*/λ they become nearly parabolic.

The present method is also used to provide results for resonant cases coming from the interaction of two modes. This occurs for

$$\kappa^2 = \frac{m \tanh H - \tanh mH}{m^2 \tanh mH - m \tanh H}, \quad m = 1, 2, 3 \ldots. \tag{22}$$

This is a generalization of the relation giving the pairs (κ, H) for which the known Wilton's failures occur. These conditions give rise to a multiplicity of solutions. For instance, two solutions could exist for $m = 2$; one is capillary-like, that is to say the wave speed decreases as the steepness increases, and the other is gravity-like with a speed that increases as the steepness increases.

For moderate depths all the waves seems to be of class I. For instance *figures 6(a)–(b)* which display plots of ε against c^2/κ corresponding to both kinds of waves computed for $m = 2$, show that the curves cut the

dashed lines which is the condition for existence of bubble-trapped limiting profiles. It should be noted that the dashed line of *figure 6(a)* merges at the right side of horizontal axis. This corresponds to limiting wave profiles having a secondary crest at $x = \pi$ with the same amplitude than the primary crests. The two limiting profiles corresponding to $m = 2$ and $h/\lambda = 0.1$, are shown in *figures 7* and *8*. For the gravity-like type, it should be noted that the center lines of the bubbles are not inclined as it was found for infinite depth but perpendicular to the line joining two crests.

5.2. Shallow water

In this subsection it will be shown that the present numerical algorithm can be used to compute solitary waves and generalized solitary waves within the framework of shallow water. Our purpose is not to give a detailed study about solitary gravity-capillary waves but to show also the capacity of the present method for computing such waves. For a review see the paper of Iooss [17], who considered the problem of capillary-gravity waves as a dynamical system.

We assume the parameter h/λ to be small but finite. This case is interesting because it provides generalized solitary waves. The approach used here deals with the bifurcation of solitary waves from infinitesimal periodic waves.

For $\kappa' = T/(\rho g h^2)$ greater than $1/3$, there exist solitary gravity-capillary waves of depression and for κ' less than $1/3$ there exist two types of waves; one type involves solitary waves of both depression and elevation with damped oscillations in the tail and the other type consists of a single crest plus a train of periodic waves of much smaller amplitude which persists at infinity. This non-local solitary wave is called generalized solitary wave. For κ' close to $1/3$, solitary waves with ripples in their tails can bifurcate from a train of infinitesimal periodic waves. We start with a small amplitude periodic wave with $d \approx H$, h/λ equal or less than 10^{-2} and κ' is close to $1/3$. As d is continuously decreased the wave profile undergoes a change of shape which gives rise to a solitary wave. For $\kappa' > 1/3$, depression waves having a very narrow trough are obtained (see *figure 9*). For $\kappa' < 1/3$, *figure 10(b)* shows a generalized solitary wave with a profile similar to those computed by Hunter and Vanden-Broeck [4]. Note that these elevation waves are intermediate states in the bifurcation from the primary infinitesimal wave of wavelength 2π to another uniform train of wavelength $2\pi/n$ where n is an integer. *Figures 10(a)–(g)*, similar to those obtained by Vanden-Broeck [18], provide a sequence of profiles which illustrate this feature. As d is decreased from its initial value, the wave troughs grow broader and the wave crests become narrow. The wave profile undergoes a sequence of modifications which gives rise to an elevation wave with a

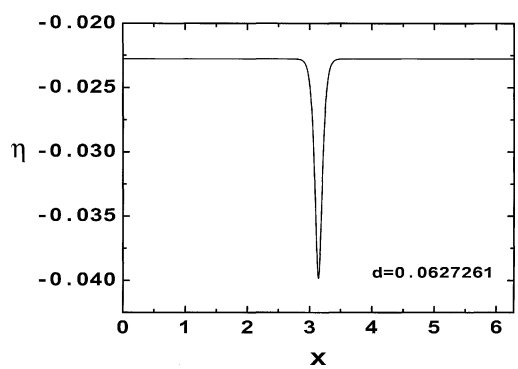

Figure 9. Typical wave profile of depression waves ($\kappa' = 1 : 2.5$, $h/\lambda = 0.01$). The vertical scale is enlarged to emphasize the behavior.

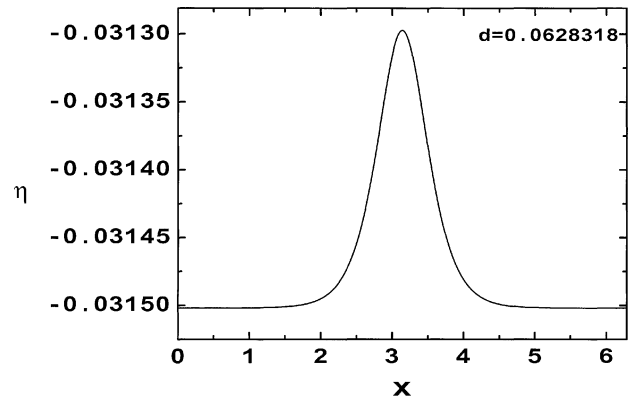

(a)

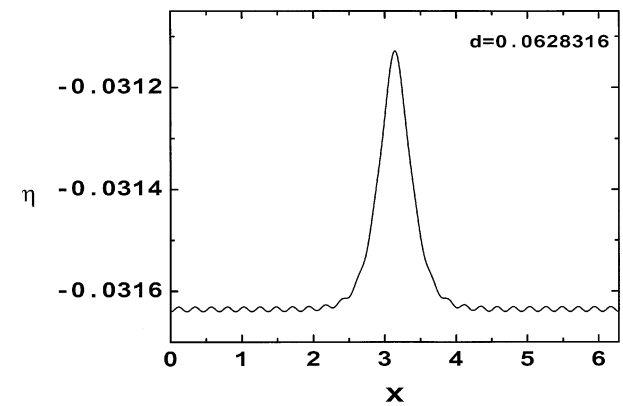

(b)

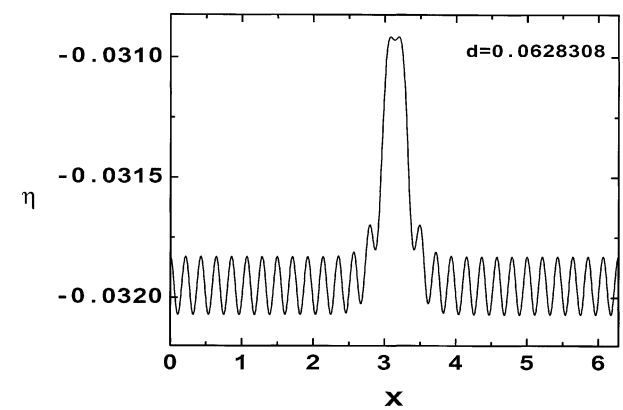

(c)

Figure 10. Sequence of profiles illustrating the bifurcation from infinitesimal wave for $\kappa' = 1 : 3.5$, $h/\lambda = 0.01$. The vertical scale is enlarged to emphasize the behavior.

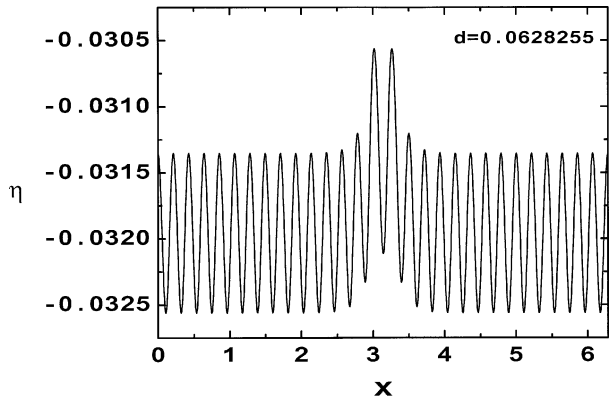

(d)

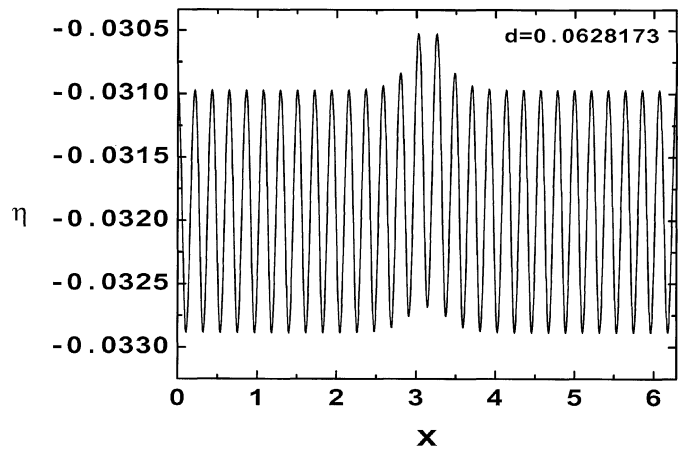

(e)

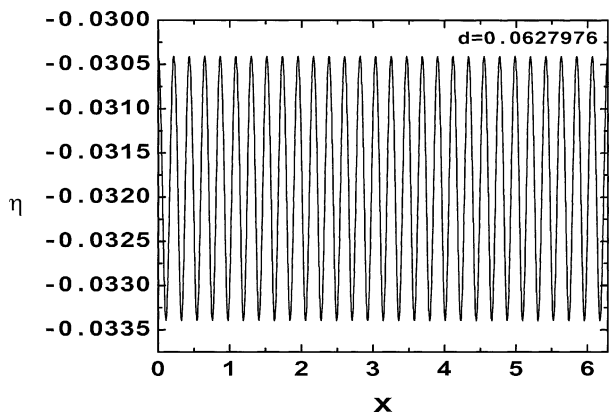

(f)

Figure 10. (Continued.)

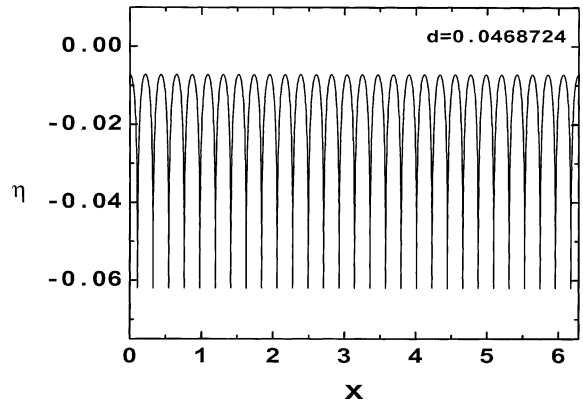

(g)

Figure 10. (Continued.)

single crest, then dimples appear and grow until the new uniform wave form is reached. We suspect that the dimples, with extremely weak amplitude, co-exist with the single crest even at the beginning of this transition.

For κ' less than $1/3$, it was observed by many authors (for more details see Grimshaw [19]) that solitary waves of elevation can co-exist with small-amplitude sinusoidal capillary waves with the same phase speed. It is the existence of this resonance that is responsible for the non-decaying tail oscillations. It can be shown from the relation (22) and $H = kh$ that $\kappa' \to 1/3$ as $H \to 0$, independently of m. Thus for small depth the interaction between two modes of different wavenumbers can generate waves presenting generalized solitary waves features.

References

[1] Kamesvara Rav J.C., On ripples of finite amplitude, Proc. Indian Ass. Cultiv. Sci. 6 (1920) 175–193.
[2] Barakat R., Houston A., Nonlinear periodic capillary-gravity waves on a fluid of finite depth, J. Geophys. Res. 184 (1968) 6546–6554.
[3] Nayfeh A. H., Finite amplitude surface waves in a liquid layer, J. Fluid Mech. 40 (1970) 671–684.
[4] Hunter J. K., Vanden-Broeck J.-M., Solitary and periodic gravity-capilary waves of finite amplitude, J. Fluid Mech. 134 (1983) 205–219.
[5] Zufiria J.A., Symmetry breaking in periodic and solitary gravity-capillary waves on water of finite depth, J. Fluid Mech. 184 (1987) 183–206.
[6] Iooss G., Kirchgassner K., Bifurcation d'ondes solitaires en présence d'une faible tension superficielle, C. R. Acad. Sci. I-Math. 311 (1990) 265–268.
[7] Dias F., Menasce D., Vanden-Broeck J.-M., Numerical study of capillary-gravity solitary waves, Eur. J. Mech. B-Fluids 15 (1996) 17–36.
[8] Jones M.C.W., Small amplitude capillary-gravity waves in a channel of finite depth, Glasgow Math. J. 31 (1987) 141–160.
[9] Kinnersley, Exact large amplitude capillary waves on sheets of fluid, J. Fluid Mech. 77 (1976) 229–241.
[10] Bloor M.I.G., Large amplitude surface waves, J. Fluid Mech. 84 (1978) 167–179.
[11] Debiane M., Kharif C., A new way for the calculation of steady periodic capillary-gravity waves on deep water, Eur. J. Mech. B-Fluids 16 (1997) 257–275.
[12] Longuet-Higgins M.S., Some new relations between Stokes's coefficients in the theory of gravity waves, J. Inst. Maths Appl. 22 (1978) 261–273.
[13] Longuet-Higgins M.S., New integral relations for gravity waves of finite amplitude, J. Fluid Mech. 149 (1984) 205–215.
[14] Balk A.M., A Lagrangian for water waves, Phys. Fluids 8 (1996) 416–420.
[15] Longuet-Higgins M.S., Lagrangian moments and mass transport in Stokes waves. Part 2. Water of finite depth, J. Fluid Mech. 186 (1988) 321–336.
[16] Hogan S.J., Some effects of surface tension on steep water waves. Part 2, J. Fluid Mech. 96 (1980) 417–445.
[17] Iooss G., Capillary-gravity water waves as a dynamical system, Proc. IUTAM/ISIMM Symposium on Structure and Dynamics of Nonlinear Waves in Fluids, World Scientific, 1995, pp. 42–47.
[18] Vanden-Broeck J.-M., Elevation solitary waves with surface tension, Phys. Fluids A3 (1991) 2659–2663.
[19] Grimshaw R.H.J, Solitary waves with oscillatory tails, Proc. IUTAM/ISIMM Symposium on Structure and Dynamics of Nonlinear Waves in Fluids, World Scientific, 1995, pp. 248–258.